NASA Cross Track Infrared Sounder (CrIS) Level 1B Delta Algorithm Theoretical Basis Document (ATBD)

University of Maryland Baltimore County Atmospheric Spectroscopy Laboratory

University of Wisconsin-Madison Space Science and Engineering Center

Version 2.1

Product Version: 2.11.1
Software Version: 2.1.3

January 2019

This research was conducted with funding provided by the National Aeronautics and Space Administration.

CrIS L1B Science and Software Team

Joe Taylor – PI	UW-Madison
Larrabee Strow – PI	UMBC
Jessica Braun	UW-Madison
Michelle Feltz	UW-Madison
Ray Garcia	UW-Madison
Robert Knuteson	UW-Madison
Graeme Martin	UW-Madison
Howard Motteler	UMBC
Greg Quinn	UW-Madison
Hank Revercomb	UW-Madison
Dave Tobin	UW-Madison

Revisions:

Draft	24 Nov 2015	Creation of initial draft document
Version 1.0Beta2	05 Febr 2016	Release consistent with Beta2 software
Version 1.0Beta3	15 Mar 2016	Release consistent with Beta3 software
Version 1.0	01 May 2017	Release consistent with 1.0 software
Version 2.0	10 May 2018	Release consistent with 2.0 software
Version 2.1	24 Jan 2019	Release consistent with 2.1 software, 2.11 product

Contacts

Readers seeking additional information about this study may contact the following researchers:

CrIS L1B Support Team cris.l1b.support@ssec.wisc.edu

Abstract

This document describes the theoretical basis of the NASA CrIS Level 1B (L1B) algorithm software and resulting product. Because the theoretical basis is very similar to that of the operational Joint Polar Satellite System (JPSS) Sensor Data Record (SDR) algorithm, it was decided to implement this document as a "delta" ATBD describing the differences between the two approaches, rather than implementing a full ATBD with duplicate information. Thus this delta ATBD together with the CrIS SDR ATBD form a complete description of the theoretical basis of the NASA CrIS L1B software.

Table of Contents

Figures

Tables

1 INTRODUCTION

1.1 Purpose of Document

This document describes the theoretical basis of the NASA CrIS Level 1B (L1B) algorithm software and resulting product.

1.2 Scope

The scope of this document is:

- Version 2.1.3 of the NASA CrIS L1B software, and
- Version 2.11.1 of the NASA CrIS L1B product

The software was developed by the CrIS L1B Science and Software Team, located at the University of Wisconsin-Madison Space Science and Engineering Center and the University of Maryland Baltimore County Atmospheric Spectroscopy Laboratory.

The product was generated by the SNPP Sounder Science Investigator-led Processing System (SIPS), located at the NASA Jet Propulsion Laboratory (JPL) and Goddard Earth Sciences Data Information Services Center (GES DISC).

1.3 Document Overview

Because the theoretical basis is very similar to that of the operational Joint Polar Satellite System (JPSS) Sensor Data Record (SDR) algorithm, it was decided to implement this document as a "delta" ATBD describing the differences between the two approaches, rather than implementing a full ATBD with duplicate information. Thus this delta ATBD together with the CrIS SDR ATBD form a complete description of the theoretical basis of the NASA CrIS L1B software.

The CrIS SDR ATBD that is a companion to this document was released December 23, 2014 by the JPSS Ground Project, and is called “Joint Polar Satellite System (JPSS) Cross Track Infrared Sounder (CrIS) Sensor Data Records (SDR) Algorithm Theoretical Basis Document (ATBD), Rev C, Code 474, 474-00032”.

The layout of this document corresponds to the layout of the CrIS SDR ATBD. Each section of this document describes the changes relative to the corresponding section in the CrIS SDR ATBD, or the words “No change” indicating there are no changes to be applied.

1.4 Reference Documents

The following references are added to the references in the CrIS SDR ATBD.

1. Joint Polar Satellite System (JPSS) Cross Track Infrared Sounder (CrIS) Sensor Data Records (SDR) Algorithm Theoretical Basis Document (ATBD), Rev C, Code 474, 474-00032

2. Joint Polar Satellite System (JPSS) Visible Infrared Imaging Radiometer Suite (VIIRS) Sensor Data Record (SDR) Geolocation Algorithm Theoretical Basis Document (ATBD), E/RA-00004, Rev. A

3. Interface Control Document between Earth Observing System (EOS) Data and Operations System (EDOS) and Science Investigator-led Processing Systems for the Suomi National Polar-Orbiting Partnership (SNPP) Science Data Segment (SDS), 423-ICD-010, Original, Earth Science Data Information Systems (ESDIS), Code 423

4. NASA SNPP Cross Track Infrared Sounder (CrIS) Level 1B Product Users' Guide, Version 2.11

5. Cross-track Infrared Sounder (CrIS) Level 1B Quality Flags Description Document, Version 2.11

6. CrIS L1B Software Users' Guide, Version 2.1

7. Montenbruck, O & Gill, Eberhard. (2000). Real-Time Estimation of SGP4 Orbital Elements from GPS Navigation Data.

8. Y. Han and Y. Chen, "Calibration Algorithm for Cross-Track Infrared Sounder Full Spectral Resolution Measurements," in IEEE Transactions on Geoscience and Remote Sensing, vol. 56, no. 2, pp. 1008-1016, Feb. 2018.doi: 10.1109/TGRS.2017.2757940

1.5 Acronyms

In addition to the acronyms defined in the CrIS SDR ATBD, the following acronyms are used throughout this document.

DM	Diagnostic Mode
EDOS	EOS Data and Operations System
EOS	Earth Observing System
FIFO	First In First Out

FSR	Full Spectral Resolution
GES DISC	Goddard Earth Sciences Data and Information Services Center
J1	NOAA-20 / JPSS-1 Satellite
JPL	Jet Propulsion Laboratory
L1A	Level 1A
L1B	Level 1B
L2	Level 2
LW	Long-wave Infrared
MW	Mid-wave Infrared
NM	Normal Mode
NSR	Normal Spectral Resolution
SIPS	Science Investigator-led Processing System
SNPP	Suomi NPP Satellite
SW	Short-wave Infrared
XSR	Extended Spectral Resolution

1.6 Notations and Symbols

Notational changes have been made to make this document self-consistent. The meanings of the symbols are defined where they are used.

2 SDR ALGORITHMS PRINCIPLES

The primary input to the L1B software is L0 data, which is composed of raw CCSDS packets as received from the spacecraft, together with added metadata. L0 data is produced and distributed by EDOS, and is equivalent to RDR data in the operational JPSS processing system. The L1B software generates L1A and L1B product files. The L1A product contains unpacked spacecraft telemetry data that has been granulated and geolocated, as well as quality flags and metadata. There is no equivalent to the CrIS L1A product in the current operational JPSS processing system. The L1B product contains calibrated spectra, together with geolocation information, quality flags, diagnostic information and metadata. L1B is equivalent to SDRs in the current operational processing system. The L1B product is used as input to L2 processing (equivalent to EDRs in the current operational processing system).

2.1 Objective of the SDR Algorithms

No change.

2.2 Space Segment Signal Processing

No change.

2.2.1 Spikes Detection/Correction

No change.

2.2.2 Filtering and Decimation

These additional figures illustrate the actual FIR filter used in the CrIS data processing and the spectral transform of it compared to a typical unfiltered signal.

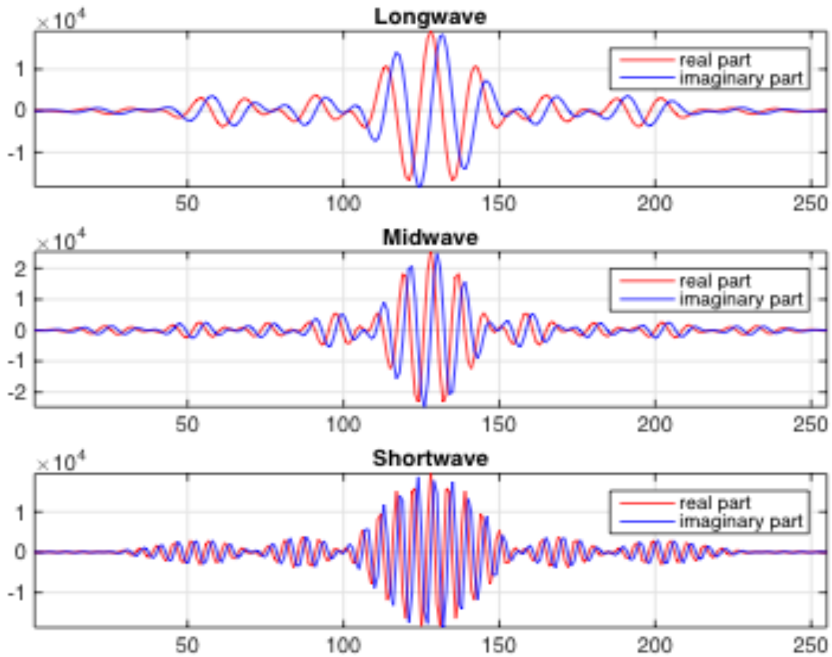

Figure 2.2.2-1 Complex FIR filters used for the CrIS sensor to suppress out of band signal and noise for each of the longwave, midwave, and shortwave bands.

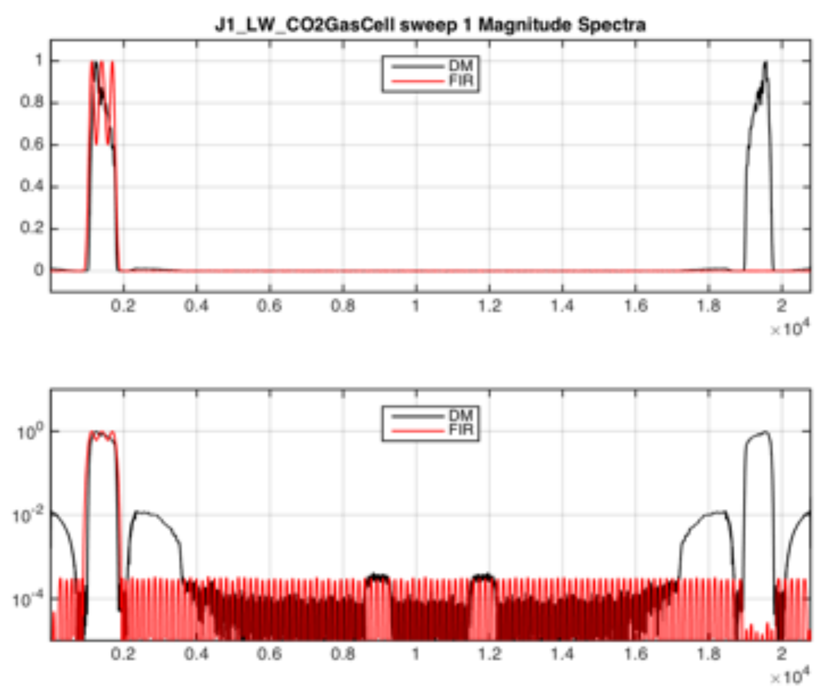

Figure 2.2.2-2 CrIS longwave band undecimated signal (DM) overlaid with FFT of corresponding FIR filter (FIR). Each curve is normalized to unity.

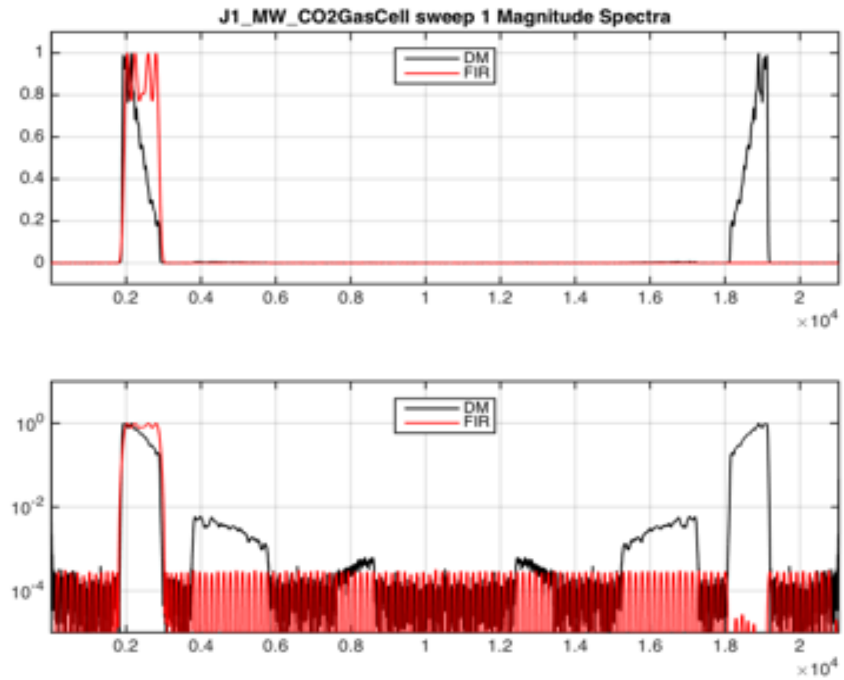

Figure 2.2.2-3 CrIS midwave band undecimated signal (DM) overlaid with FFT of corresponding FIR filter (FIR). Each curve is normalized to unity.

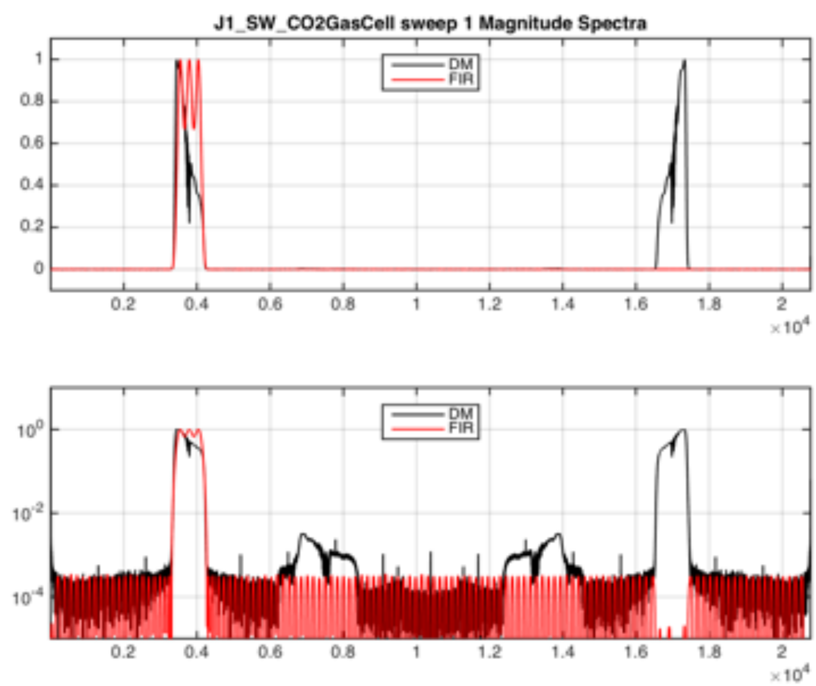

Figure 2.2.2-4 CrIS shortwave band undecimated signal (DM) overlaid with FFT of corresponding FIR filter (FIR). Each curve is normalized to unity.

2.2.3 Bit Trimming

No change.

2.2.4 Packet Encoding

No change.

2.3 Ground Segment Processing

No change.

2.4 Interferometer Model

No change.

2.4.1 Instrument Phase

No change.

2.4.2 Other Signal Contributors

No change.

2.4.3 Instrument Line Shape

No change.

2.4.4 Other Types of Errors

No change.

2.4.5 Interferometer Modeling Equations

No change.

2.5 CrIS Characteristics

No change.

2.5.1 Double-Sided Interferogram Measurements

No change.

2.5.2 CrIS Spectral Bands

For the first part of the SNPP mission, the effective spectral resolution of CrIS data received from the satellite was lower in the short-wave and mid-wave infrared bands than in the long-wave infrared band. Level 0 data received during this initial period is referred to as Normal Spectral Resolution (NSR). Table 2 and Figure 14 in the SDR ATBD correctly state the spectral sampling of the calibrated radiances for the original low resolution SNPP CrIS data collection mode.

On 4 December 2014 (15:06 UTC), the resolution of the short-wave and mid-wave data transmitted from the SNPP satellite was increased to match the long-wave resolution. Level 0 data received during this period is referred to as Full Spectral Resolution (FSR). After the transition to FSR, the effective spectral resolution of short-wave data received on the ground was quadrupled, and the effective spectral resolution of mid-wave data was doubled, with the Level 0 data volume increasing accordingly.

On 2 November 2015 (16:06 UTC), the SNPP satellite began transmitting long-wave and short-wave interferograms with extra points on the ends. These points had previously been discarded, but were added to the data stream because it was determined that they could be used to improve the quality of the calibration for the FSR radiances. Level 0 data received during this period is referred to as Extended Spectral Resolution (XSR).

The J1 satellite has transmitted CrIS data at XSR for the entire mission to date.

The SNPP-only Version 2.0 L1B product includes datasets at two different spectral resolutions, to meet the goals of providing a spectrally consistent product with the longest possible duration and also with the highest possible spectral resolution. These L1B datasets are referred to as NSR and FSR. The J1-only Version 2.11 L1B dataset is produced only at FSR.

For more information on the resolution of the CrIS L1B product datasets, refer to the NASA CrIS L1B Product Users Guide, Version 2.11.

2.5.3 CrIS Field of Regard

No change.

2.5.4 CrIS Measurement Sequence

No change.

2.5.5 CrIS Signal Processing

The SDR ATBD Table 4 represents the interferogram number of points at launch of SNPP during the NSR data collection period. The following table summarizes the interferogram data processed using the NASA CrIS L1B software as described in Section 2.5.2 of this document. The label DM (Diagnostic Mode) indicates the number of interferogram points prior to the on-orbit application of the FIR filter (see Section 2.2.2). The label NM (Normal Mode) indicates the number of interferogram points output by the FIR filter and downlinked from the satellite to the ground.

Table 2.5.5- 1 Number of interferogram points before and after on-board filtering.

CrIS Data Mode	LW	MW	SW
NM SNPP NSR	866	530	202
NM SNPP FSR	866	1052	799
NM SNPP XSR	874	1052	808
NM JPSS1 XSR	876	1052	808
Decimation Factor	24	20	26
DM SNPP NSR	866*24+254	530*20+254	202*26+254
DM SNPP FSR	866*24+254	1052*20+254	799*26+254
DM SNPP XSR	874*24+254	1052*20+254	808*26+254
DM JPSS1 XSR	876*24+254	1052*20+254	808*26+254

2.6 Signal Representation

No change.

2.6.1 Array Dimensions

No change.

2.6.2 Data Ordering

No change.

3 SPECIAL CONSIDERATIONS

3.1 Non-linearity Correction

No change.

3.2 Scan Mirror Polarization Compensation

A correction for scan mirror angle polarization is anticipated but no polarization correction has been implemented in the current version.

3.3 Fringe Count Error Handling

No fringe count error detection or correction is currently included in the NASA L1B processing. The correction algorithm described in the ATBD was not included, as it is not yet needed for the CrIS data processing since there have been no fringe count errors during routine operation.

3.3.1 Phase Analysis

Not implemented; no fringe count errors detected for CrIS.

3.3.2 Spectrum Based Detection and Correction

Not implemented; no fringe count errors detected for CrIS.

3.3.3 FCE Detection

Not implemented; no fringe count errors detected for CrIS.

3.3.4 FCE Correction

Not implemented; no fringe count errors detected for CrIS.

3.4 Lunar Intrusion Handling

3.4.1 Lunar Intrusion Detection

"*On rare instances, the space look measurement used to calibrate the CrIS sensor background may encounter a view of the moon. Typically, this may only occur on one or two FOVs simultaneously and possibly on 2 to 3 successive space looks as the spacecraft orbit progresses past the view of the moon. When this happens, then it is necessary to detect this condition and exclude use of this contaminated space look data in the CrIS calibration.*" [CrIS SDR ATBD].

Lunar intrusion detection is completed by comparing the uncalibrated spectrum for any new Deep Space scene versus a reference Deep Space mean that is ideally free of lunar intrusion effects. This is completed independently for all 27 CrIS detectors (9 FOVs in 3 detector bands) and interferometer sweep direction.

The following steps are taken to detect a lunar intrusion. Deep Space and ICT spectra from the context granules are included in the process when context granules have been provided to the processing. The use of context granules is expected to provide more robust lunar intrusion detection.

1. Iterative detection of Deep Space spectra outliers with respect to the mean Deep Space spectra. Complete three iterations of the following steps a - f:
    a. Calculate Deep Space uncalibrated (complex) spectral average (in band "b", FOV "p", and sweep direction "d", averaged over scan "k"), with outliers removed (no outliers flagged for first iteration), $\left\langle \tilde{S}^{ds}_{b,p,d}[n,k] \right\rangle_k$
    b. Calculate the ICT uncalibrated spectral average (no outlier detection), $\left\langle \tilde{S}^{ict}_{b,p,d}[n,k] \right\rangle_k$.
    c. Subtract the Deep Space uncalibrated (complex) spectral average with outliers removed (1.a) from the individual Deep Space uncalibrated (complex) spectra:
    $$\tilde{R}^{ds}_{b,p,d}[n,k] = \tilde{S}^{ds}_{b,p,d}[n,k] - \left\langle \tilde{S}^{ds}_{b,p,d}[n,k] \right\rangle_k \quad [3.4.1]$$
    d. Subtract the Deep Space uncalibrated (complex) spectral average with outliers removed (1.a) from the ICT uncalibrated spectral average (1.b):
    $$\tilde{R}^{ict}_{b,p,d}[n] = \left\langle \tilde{S}^{ict}_{b,p,d}[n,k] \right\rangle_k - \left\langle \tilde{S}^{ds}_{b,p,d}[n,k] \right\rangle_k \quad [3.4.2]$$
    e. Compute the magnitude of the complex ratio of [3.4.1] to [3.4.2], averaged over the spectral channels limited by the spectral channel indices provided in Table 3.4.1-1 ($n_{\min}$ and $n_{\max}$ define the wavenumber bins corresponding to the lower and upper limits of the spectral band average, respectively):
    $$C^{ds}_{b,p,d}[k] = \frac{\left| \sum_{n=n_{\min}}^{n_{\max}} \frac{\tilde{R}^{ds}_{b,p,d}[n,k]}{\tilde{R}^{ict}_{b,p,d}[n]} \right|}{n_{\max} - n_{\min}} \quad [3.4.3]$$
    f. Compare [3.4.3] to its mean. Index values that exceed a 3-σ deviation from the mean. Deep Space views corresponding to these indices are considered outliers, and are removed from subsequent mean Deep Space reference calculations within

the lunar detection algorithm.

2. Calculate Deep Space uncalibrated (complex) spectral average (in band “b”, FOV “p”, and sweep direction “d”), with outliers identified in Step 1 removed.
3. Calculate the ICT uncalibrated spectral average (no outlier detection).
4. Subtract the Deep Space uncalibrated (complex) spectral average with outliers removed from the individual Deep Space uncalibrated (complex) spectra (Eq. [3.4.1]).
5. Subtract the Deep Space uncalibrated (complex) spectral average with outliers removed from the ICT uncalibrated spectral average (Eq. [3.4.2]).
6. Compute the magnitude of the complex ratio of [3.4.1] to [3.4.2], averaged over the spectral channels limited by the spectral channel indices provided in Table 3.4.1-1 (Eq. [3.4.3]).
7. Compute $\left\langle C^{ds}_{b,p,d}\left[k_{good}\right]\right\rangle$, the mean of Eq. [3.4.3] with scans corresponding to outliers identified in Step 1 removed from $\tilde{R}^{ds}_{b,p,d}$:

$$C^{ds}_{b,p,d}\left[k_{good}\right]=\frac{\left|\sum_{n=n_{\min}}^{n_{\max}}\frac{\tilde{R}^{ds}_{b,p,d}\left[n,k_{good}\right]}{\tilde{R}^{ict}_{b,p,d}\left[n\right]}\right|}{n_{\max}-n_{\min}} \qquad [3.4.4]$$

8. Compare [3.4.3] to the sum of $\left\langle C^{ds}_{b,p,d}\left[k_{good}\right]\right\rangle$ and the band dependent threshold (Table 3.4.1-2). Index values that exceed the sum. Deep Space views corresponding to these indices are flagged positive for lunar intrusion detection.

$$LI_{b,p,d}\left[k\right]=\begin{cases}0, & C^{ds}_{b,p,d}\le\left\langle C^{ds}_{b,p,d}\left[k_{good}\right]\right\rangle+\dfrac{LI_{\lim}}{100}\\ 1, & C^{ds}_{b,p,d}>\left\langle C^{ds}_{b,p,d}\left[k_{good}\right]\right\rangle+\dfrac{LI_{\lim}}{100}\end{cases} \qquad [3.4.5]$$

The lower and upper limits for the averages over spectral channel are provided in Table 3.4.1-1. The threshold values used for lunar detection are provided in Table 3.4.1-2.

Table 3.4-1 Lower and upper channel limits for the averages over spectral channel used in the lunar intrusion detection algorithm.

Detector Band	**Lower Limit (cm^{-1})**	**Upper Limit (cm^{-1})**
LW	750	995
MW	1310	1650
SW	2255	2450

Table 3.4-2 Threshold values used for lunar detection.

Detector Band	**Lunar Intrusion Threshold (%)**
LW	0.9
MW	1.2
SW	1.8

3.4.2 Lunar Intrusion Processing

If equation [3.4.5] is true for any specific band, FOV, and sweep direction, then the Deep Space spectrum is marked as invalid only for that band, FOV, and sweep direction. Any deep space measurements marked invalid from this process are excluded from the Moving Window average and the lunar intrusion flag is also set. Earth scenes calibrated using a Deep Space Moving Window average for which Deep Space views have been removed due to a lunar intrusion detection are also marked with a lunar intrusion quality flag.

3.5 Alignment of Data to a Common Spectral Grid

The primary change for the NASA L1B processing, with respect to CrIS SDR ATBD Section 3.5, is that spectral resampling is performed on the *undecimated* spectral domain.

The F-matrix operator is defined as:

$$F[k,k'] = \frac{\Delta\sigma_s}{\Delta\sigma_u} \frac{\mathrm{Sin}(\pi \frac{\sigma_{s,k'} - \sigma_{u,k}}{\Delta\sigma_u})}{N_O \mathrm{Sin}(\pi \frac{\sigma_{s,k'} - \sigma_{u,k}}{N_O \Delta\sigma_u})} \quad [3.5.1]$$

where,

$\Delta\sigma_s$ is the sensor spectral grid spacing,

$\Delta\sigma_u$ is the user spectral grid spacing,

$\sigma_{s,k'}$ is the wavenumber for the bin k' on the sensor grid σ_s,

$\sigma_{u,k}$ is the wavenumber for the bin k on the user spectral grid σ_u , and

N_O is the undecimated number of interferogram samples truncated to NSR MOPD (N_O = 20736 for the LW, N_O = 10560 for the MW, and N_O = 5200 for the SW).

The band dependence of the F-operator, $\Delta\sigma_s$, and $\Delta\sigma_u$ is not explicitly noted in equation [3.5.1]. The F-matrix operator is computed separately for each granule using Neon data contained in the most coincident engineering packet.

Wavenumbers assigned to each spectral bin prior to resampling are based on the laser metrology sampling wavelength (see Section 4.1 of the ATBD). The laser λ_L^b value in band "b" is computed by the spectral calibration module and used to recompute the F-matrix operator (based on the calibration neon count). The laser wavelength is stabilized on the CrIS instrument (λ_L^b stable to within +/-0.4 ppm over one orbit).

3.6 ILS Correction

No change.

3.6.1 Introduction

No change.

3.6.2 CrIS Off-Axis Self Apodization

No change.

3.6.3 Self-Apodization Removal

Numerical evaluation of the integral

The Self-Apodization (SA) matrix is calculated as:

$$SA[k',k] = \int_{\sigma_{\min}}^{\sigma_{\max}} d\sigma' \, \mathrm{Psinc}\left(\frac{\sigma_{k'} - \sigma'}{\Delta\sigma_s}, N_O\right) \cdot ILS(\sigma', \sigma_k) \qquad [3.6.1]$$

where,

$$\mathrm{Psinc}(x, N_O) = \frac{\sin(\pi x)}{N_O \sin\left(\pi x / N_O\right)} \qquad [3.6.2]$$

$\Delta\sigma_s$ is the sensor spectral grid spacing

σ_k is the wavenumber for the bin k,

N_O is the undecimated number of interferogram samples truncated to L0 NSR MOPD for the L1B NSR product (N_O = 20784 for the LW, N_O = 10600 for the MW, and N_O = 5252 for the SW), or at the L0 XSR MOPD for the FSR L1B product (N_O = 20976 for the LW, N_O = 21040 for the MW, and N_O = 21008 for the SW)

$ILS(\sigma', \sigma_k)$ is the self apodized instrument line shape distortion due to off axis geometry.

Equation [3.6.1] replaces Equation [41] of the CrIS SDR ATBD (Rev C).

The numerical calculation of the SA matrix described by Equations [3.6.1] and [3.6.2] can create spectral ringing artifacts at the band edges when the wavenumber scale indices k and k’ match the number of number of output channels after inversion. To mitigate this effect, a temporary expanded square self-apodization (SA) matrix is used, denoted by SA*. The size of SA* is the number of interferogram points multiplied by an expansion factor, with the center of the SA and

SA* wavenumber scales aligned. An expansion factor of 3.0 is used for all 3 bands (LW, MW, and SW) when generating the inverse self-apodization matrix. The inverse of the expanded SA* matrix is calculated, and SA^{-1} is extracted from SA^{*-1}. The use of an expansion factor is described in Han and Chen (2018), in Section IV of "Calibration Algorithm for Cross-Track Infrared Sounder Full Spectral Resolution Measurements" (DOI: 10.1109/TGRS.2017.2757940).

The inverse self apodization matrix is calculated offline for each band "b" using a nominal laser metrology sampling wavelength value, $\lambda_{L,ISA}^{b}$. The current laser metrology sampling wavelength for band "b" (λ_{L}^{b}) is determined from the spectral calibration module (based on the neon count). If λ_{L}^{b} differs from $\lambda_{L,ISA}^{b}$ by more than a pre-defined threshold, the ISA degraded QF is set to 1.

3.6.4 Residual Term

The residual term is not calculated.

3.6.5 Guard Band Damping

The calibration filter formulation is the same as that described in the CrIS SDR ATBD document:

$$f_b[k] = \left[\frac{1}{e^{a_2(k_0-a_1-k)}+1}\right]\cdot\left[\frac{1}{e^{a_4(k-k_1-a_3)}+1}\right] \quad [3.6.3]$$

The parameters for the filter have been optimized for use within the NASA L1B complex calibration procedure. The parameters are provided in Table 3.6.5-1.

To be independent of wave number, equation [3.6.3] is expressed in bins. It is important to note that the bin number range begin at 1, and not at zero. In case the range starts at 0, the three k 's in Table 3.6.5-1 need to be reduced by 1.

Table 3.6.5-1 Parameters for the calibration filter $f_b[k]$. NSR and FSR denote L1B product output resolution.

	LW	MW	SW
k	1 - 866 (NSR) 1 - 874 (SNPP FSR) 1 - 876 (J1 FSR)	1 - 530 (NSR) 1 - 1052 (FSR)	1 - 202 (NSR) 1 - 808 (FSR)
k_0	57 (NSR) 59 (FSR)	48 (NSR) 80 (FSR)	20 (NSR) 83 (FSR)

k_1	777 (NSR) 785 (SNPP FSR) 787 (J1 FSR)	494 (NSR) 988 (FSR)	185 (NSR) 747 (FSR)
a_1	21 (NSR) 22 (FSR)	7 (NSR) 35 (FSR)	10 (NSR) 35 (FSR)
a_2	1.0	2.0 (NSR) 0.5 (FSR)	4.0 (NSR) 0.5 (FSR)
a_3	54 (NSR) 55 (FSR)	7 (NSR) 35 (FSR)	8 (NSR) 35 (FSR)
a_4	1.0	2.0 (NSR) 0.5 (FSR)	4.0 (NSR) 0.5 (FSR)

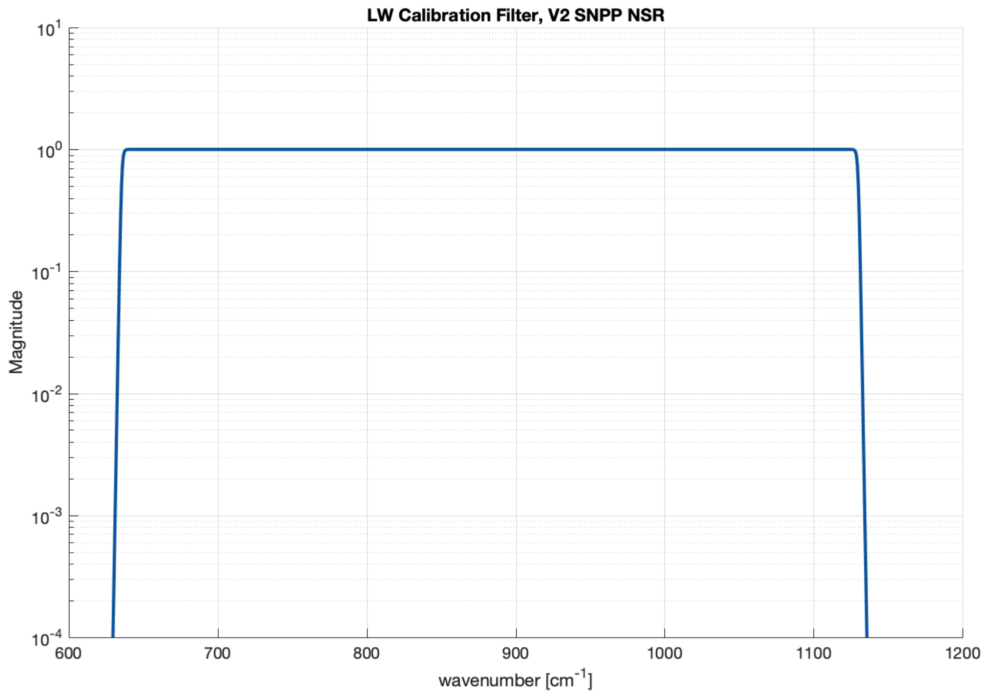

Figure 3.6.5-1 Calibration filter for LW band (SNPP, NSR).

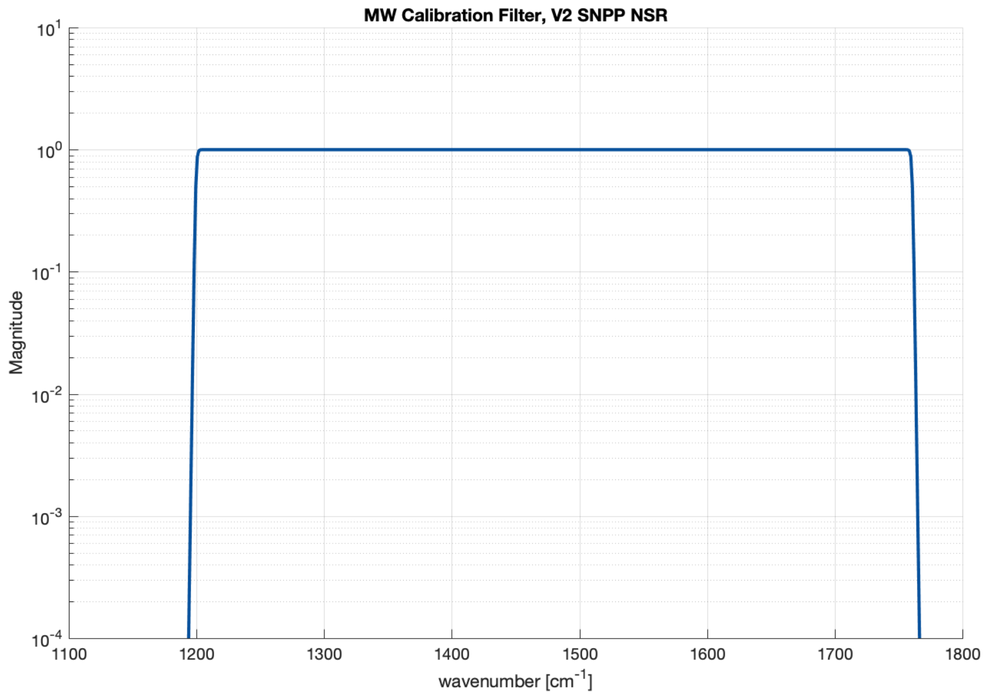

Figure 3.6.5-2 Calibration filter for MW band (SNPP, NSR).

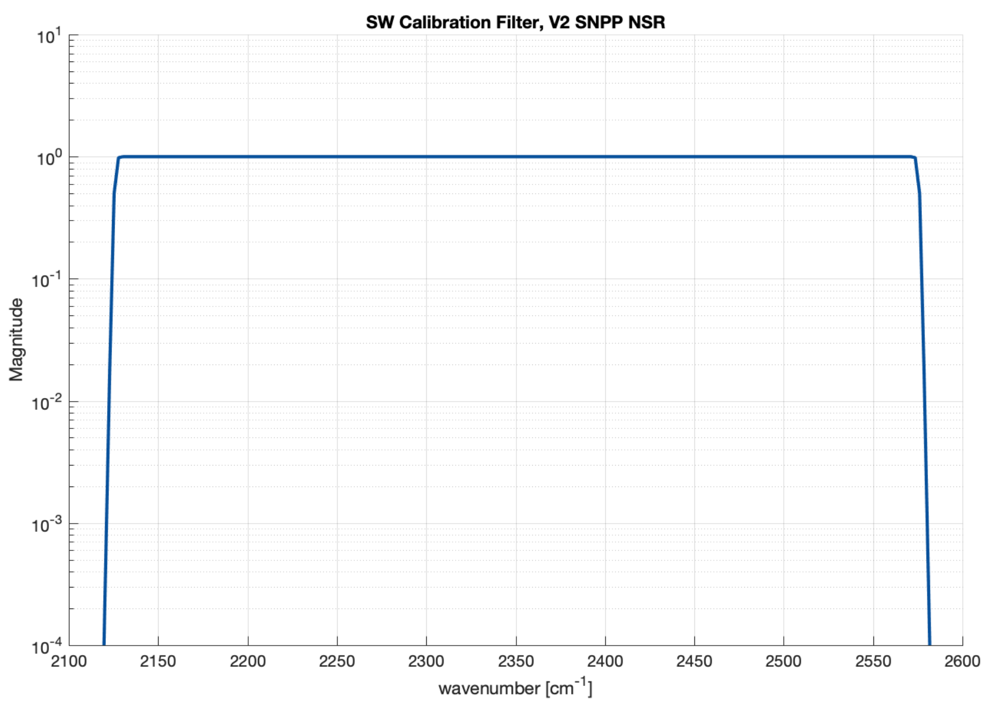

Figure 3.6.5-3 Calibration filter for SW band (SNPP, NSR).

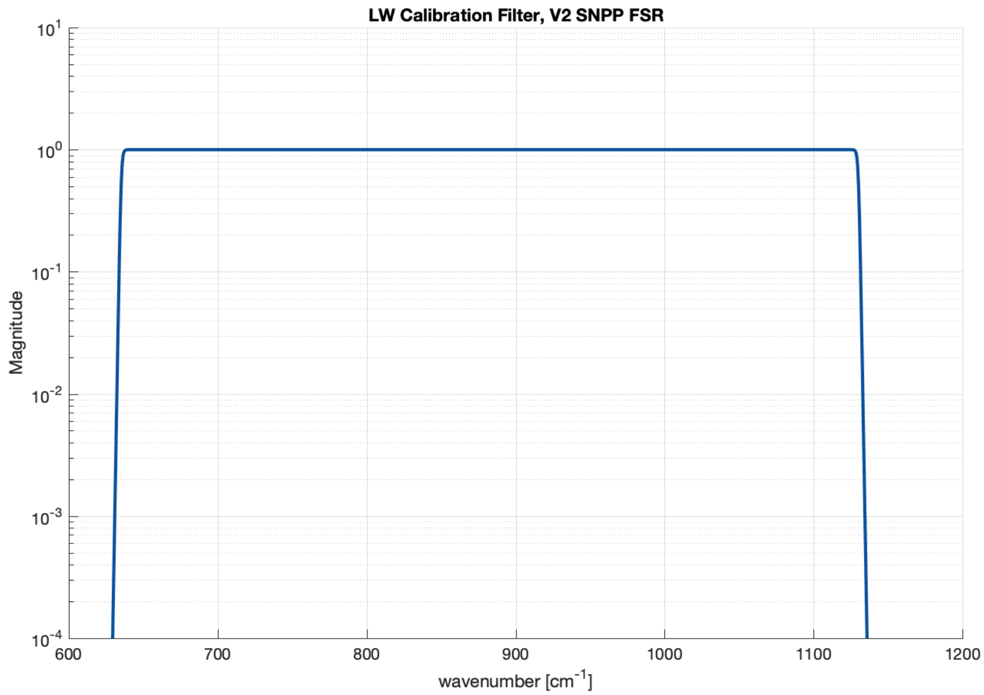

Figure 3.6.5- 4 Calibration filter for LW band (SNPP, FSR).

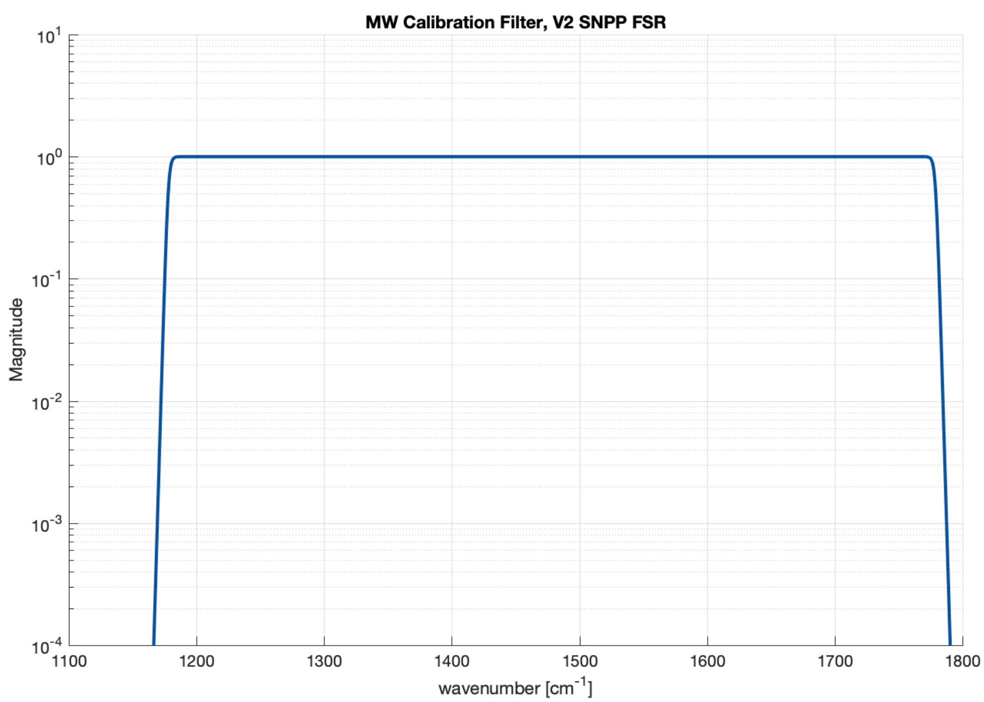

Figure 3.6.5- 5 Calibration filter for MW band (SNPP, FSR).

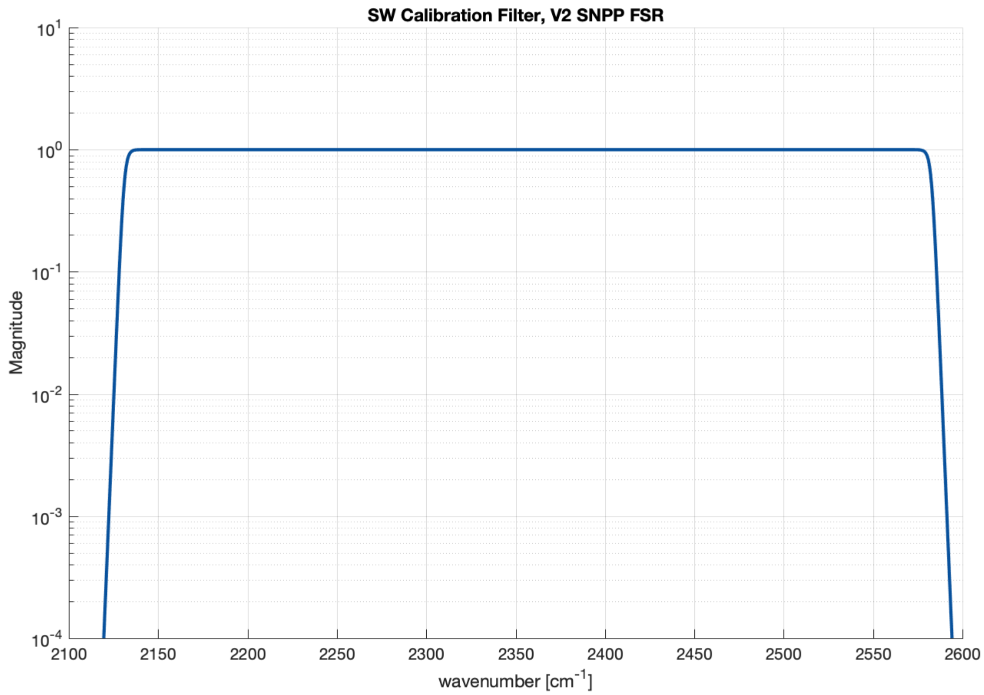

Figure 3.6.5- 6 Calibration filter for SW band (SNPP, FSR).

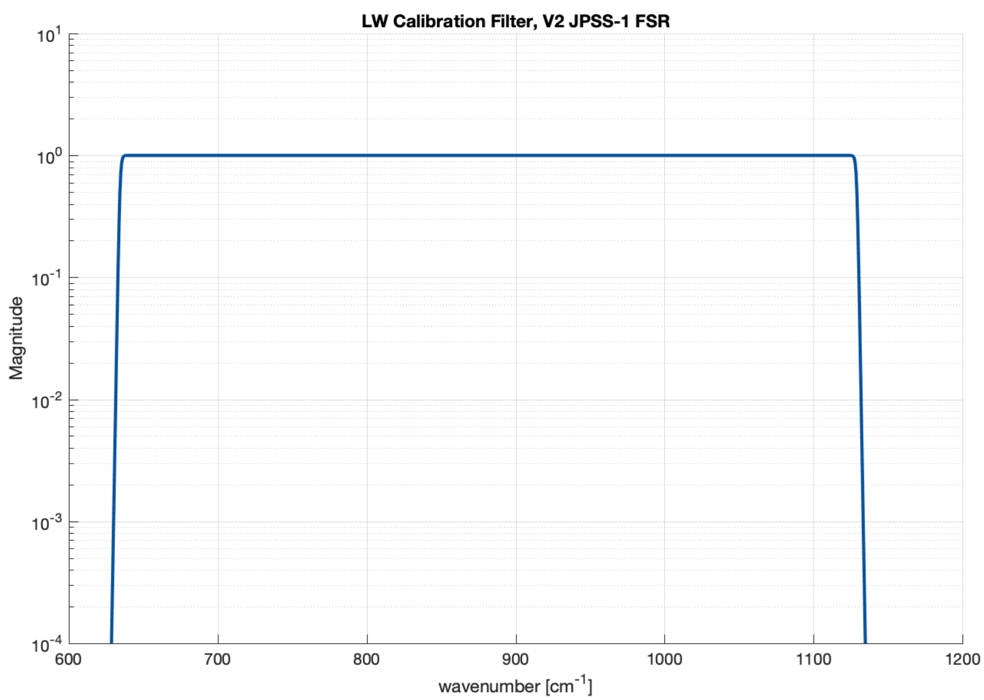

Figure 3.6.5- 7 Calibration filter for LW band (J1, FSR).

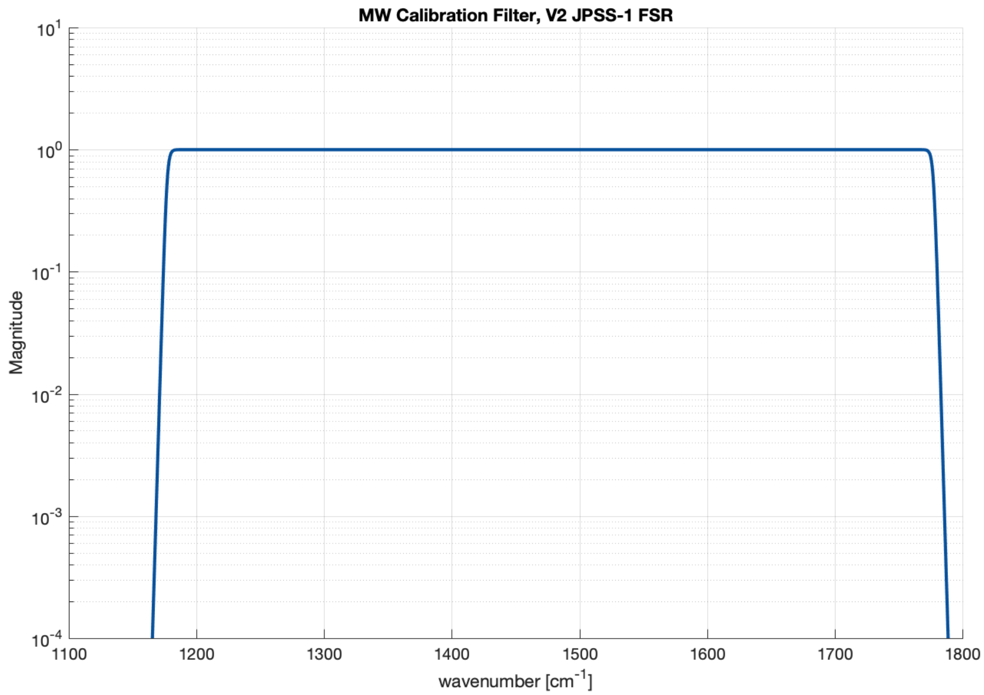

Figure 3.6.5- 8 Calibration filter for MW band (J1, FSR).

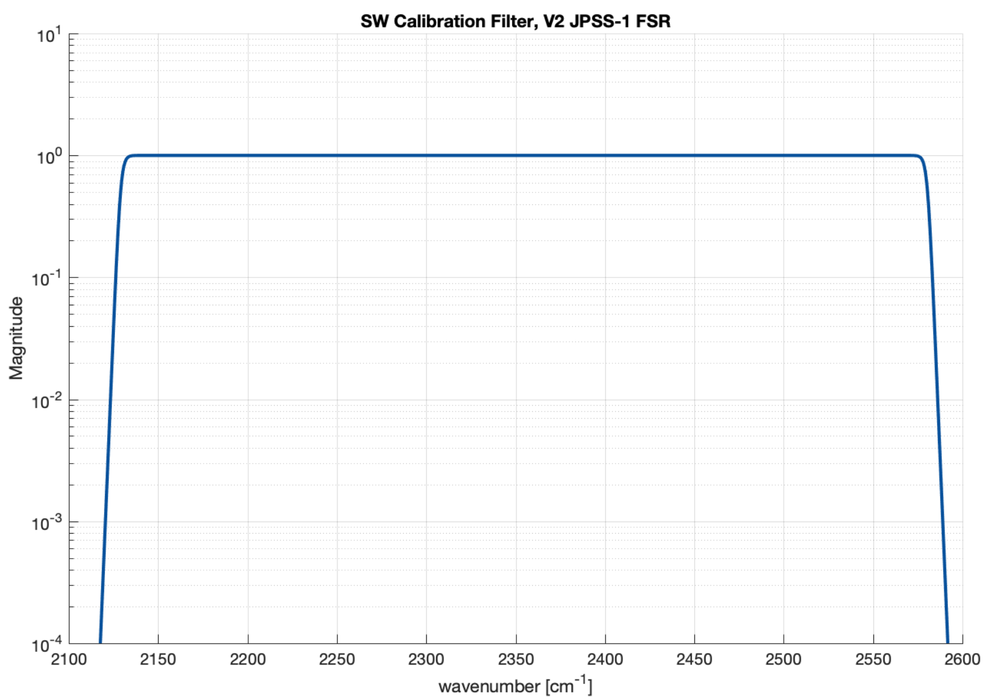

Figure 3.6.5- 9 Calibration filter for SW band (J1, FSR).

3.6.6 ILS Retrieval

The spectral calibration of the instrument is impacted by optical alignments and FOV geometry (FOV size, shape, geometry and off-axis angles). The ILS retrieval process has been designed to identify the FOV dependent parameters required to construct inverse self-apodization matrices that provide optimal correction of the self-apodization of all 27 detector channels.

The process utilizes knowledge of the FOV size, shape, geometry and off-axis angles for each FOV obtained from instrument design and instrument characterization (conducted during TVAC and on-orbit).

3.7 Signal Apodization

Unapodized radiances are output for the standard L1B product.

3.7.1 Unapodized Channel Response Function

No change.

3.7.2 Hamming's Filter Function

The spectral operators (bandguard filter, spectral resampling, self-apodization removal, and Hamming apodization are not combined into a single CMO matrix.

3.7.3 Blackman-Harris's Apodization Function

No change.

3.8 CMO Updates

The spectral operators (bandguard filter, spectral resampling, self-apodization removal, and Hamming apodization are not combined into a single CMO matrix.

4 SPECTRAL CALIBRATION

4.1 Neon-lamp as a Spectral Reference

No change.

4.1.1 Wavelength Calculation

No change.

4.1.2 Calculation of Laser Metrology Wavelength

No change.

4.1.3 Rejecting Bad Neon Count Measurements (Quality Control)

No change.

4.2 Metrology Wavelength Monitoring

No change.

5 RADIOMETRIC CALIBRATION

5.1 Basic Radiometric Relations

No change.

5.2 General Calibration Equation

No change.

5.3 CrIS Specific Calibration Equation

The CrIS specific calibration equation, as implemented by the NASA L1B CrIS processing, using notation consistent with Section 5.3 of the CrIS SDR ATBD, is written:

$$L^S_{b,p,d} = L^H \cdot \frac{F_b \cdot f_b \cdot SA^{-1}_{b,p} \cdot f_b \cdot \left[\frac{\Delta S_1}{\Delta S_2} \left| \Delta S_2 \right| \right]}{F_b \cdot f_b \cdot SA^{-1}_{b,p} \cdot f_b \cdot \left| \Delta S_2 \right|} \qquad [5.3.1]$$

$$\Delta S_1 = \left(\tilde{S}^S_{b,p,d} - \left\langle \tilde{S}^C_{b,p,d} \right\rangle \right) \qquad [5.3.2]$$

$$\Delta S_2 = \left(\left\langle \tilde{S}^H_{b,p,d} \right\rangle - \left\langle \tilde{S}^C_{b,p,d} \right\rangle \right) \qquad [5.3.3]$$

where,

$L^S_{b,p,d}$ is the calibrated scene radiance

$\tilde{S}^S_{b,p,d}$ are the complex uncalibrated Earth scene spectra as measured by the instrument,

$\tilde{S}^C_{b,p,d}$ are the complex uncalibrated cold reference (Deep Space) spectra as measured by the instrument (complex),

$\tilde{S}^H_{b,p,d}$ are the complex uncalibrated hot reference (ICT) spectra as measured by the instrument (complex),

L^H is the calculated radiance for the hot calibration reference (the ICT), calculated on the user wavenumber scale

F_b is the spectral resampling matrix operator,

f_b is the band calibration filter matrix operator,
$SA^{-1}_{b,p}$ is the Self Apodization removal matrix operator,
b, p, and d denote band, field of view, and sweep direction dependence, respectively.

For reference, the CrIS specific calibration Eq. 72 presented in the CrIS SDR ATBD is included here:

$$L^S = F^{-1}_{INT} \cdot \left[\frac{\tilde{S}^S - \langle \tilde{S}^C \rangle}{\langle \tilde{S}^H \rangle - \langle \tilde{S}^C \rangle} \right] \cdot F_{INT} L^H + F^{-1}_{INT} \cdot \left[\frac{\langle \tilde{S}^H \rangle - \tilde{S}^S}{\langle \tilde{S}^H \rangle - \langle \tilde{S}^C \rangle} \right] \cdot F_{INT} L^C \quad [5.3.4]$$

As noted in the CrIS SDR ATBD, during normal on-orbit operation the cold reference radiance $L_C = 0$ so that the second term in equation [5.3.4] can be ignored resulting in a further simplification:

$$L^S = F^{-1}_{INT} \cdot \left[\frac{\tilde{S}^S - \langle \tilde{S}^C \rangle}{\langle \tilde{S}^H \rangle - \langle \tilde{S}^C \rangle} \right] \cdot F_{INT} L^H \quad [5.3.5]$$

In the CrIS SDR ATBD implementation, the F^{-1}_{INT} term in equation [5.3.4] is combined into the CMO (Correction Matrix Operator) matrix. The CrIS SDR ATBD as defines the CMO matrix:

$$CMO_{b,p} = H_b \cdot R^{-1}_{b,p} \cdot SA^{-1}_{b,p} \cdot F_b \cdot f_b \quad [5.3.6]$$

where,
H_b is the Hamming apodization matrix operator, and
$R^{-1}_{b,p}$ residual ILS removal matrix operator.

Omitting the Hamming apodization and residual ILS removal from [5.3.6], the CrIS SDR ATBD CrIS specific calibration equation (Eq. [5.3.5]) can be rewritten in a form that can be more easily compared with the NASA L1B CrIS Calibration Equation [5.3.1]:

$$L^S = SA^{-1}_{b,p} \cdot F_b \cdot f_b \cdot \left[\frac{\tilde{S}^S - \langle \tilde{S}^C \rangle}{\langle \tilde{S}^H \rangle - \langle \tilde{S}^C \rangle} \right] \cdot F_{INT} L^H \quad [5.3.7]$$

5.4 ICT Radiometric Model

No change.

5.4.1 Radiometric Error

No change.

5.4.2 Radiometric Model Formulation

The ICT radiometric model is calculated on the user wavenumber grid. Accordingly, the spectrally resolved parameters in Table 14 are on the user wavenumber grid.

The J1 Internal Calibration Target (ICT) has much higher emissivity than the SNPP ICT. In addition, the J1 ICT is a specular trap while the SNPP ICT is a diffuse cylindrical cavity. Equations 74a through 78c are used for for the radiometric model of both ICT designs, but view factors are sensor dependent. All of the view factors, except for the view to the cold beamsplitter, for the J1 ICT radiometric model are set to zero. Replace Table 15 in the reference ATBD with Table 5.4.2-1 below.

Table 5.4.2- 1 Fraction of view from ICT bottom surface to each environment surface (notional).

View from	To	SNPP Fractional View to Environment	J1 Fractional View to Environment
ICT Base	ICT Walls	-	-
ICT Base	ICT Base	-	-
ICT Base	ICT Baffle	0.175	0
ICT Base	Scan Baffle	0.508	0
ICT Base	Frame	0.214	0
ICT Base	Opto-Mechanical Assembly		
ICT Base	Warm Beamsplitter	0.086	0
ICT Base	Cold Beamsplitter	0.008	1
ICT Base	Space	0.009	0

5.5 ICT Temperature Computation

No change.

5.6 Signal Coaddition

N^{ma} = 29 for the DS and ICT signal coaddition.

5.6.1 Moving Average

The Earth Scene (ES) views in each scan line are calibrated using reference Deep Space (DS) and Internal Calibration Target (ICT) views from the current and adjacent scan lines if they are available. In the optimal situation, reference views from the 14 preceding scan lines and the 14 following scan lines will be used, in addition to the reference views from the current scan line. However, the calibration will still be performed if as few as one reference view of each type is available. If a calibration is performed with fewer than the optimal number of reference views, for example due to a data drop-out or an instrument change, the noise in the calibrated ES spectra will be elevated. If there are 24 or more views in the moving average, the radiometric calibration quality flag will be set to 'No issues detected' (value = 0), if there are between 19 and 24 views in the moving average, the radiometric calibration quality flag will be set to 'good' (value = 1), and if there are 19 or fewer views in the moving average, the radiometric calibration quality flag will be set to 'invalid' (value = 2).

5.6.2 Impact of Temperature Drift

No change.

5.6.3 Throughput Delay

No change.

6 GEOMETRIC CALIBRATION

The NASA L1B software includes a new geolocation implementation based on the approach outlined in the CrIS SDR ATBD and the VIIRS SDR Geolocation ATBD. The CrIS SDR ATBD describes the sensor dependent portion of geolocation (line of sight vector calculation from instrument telemetry) and the VIIRS SDR ATBD describes the sensor independent part (earth location from sensor line of sight).

L1B geolocation fields are additionally adjusted to account for terrain. This is done using the approach described in the VIIRS SDR ATBD (which applies to VIIRS SDRs but not CrIS SDRs). The digital elevation model (DEM) used for L1B terrain correction and field-of-view geography (see below) is the equal-angle 30 arcsecond model made available as part NASA's SDP toolkit. For latitudes beyond +/- 70 degrees, the DEM has been resampled to a pair of azimuthal equal-area projections at 1 km resolution covering the north and south poles.

The L1B product includes a number of geolocation fields beyond those provided in SDR geolocation. A brief outline on how a number of these fields are derived is provided below.

Field of View Extent and Geography

lat_bnds, lon_bnds, land_frac, surf_elev, surf_elev_sdev

The L1B product includes for each observation a series of 8 locations that describe the perimeter of the FOV's intersection with the earth's surface, accounting for terrain. These are based on the longwave FOV angular diameter values that come from the CrIS engineering packet. (All other FOV-specific constants use for geolocation reference the longwave values, consistent with the CrIS SDR ATBD.)

The angular diameter values are further used to find points from the DEM that are within the spatial extent of the observation, which are then aggregated to provide land fraction and surface elevation statistics. Testing each DEM point for inclusion is done via a dot product threshold test between the satellite to FOV center vector and satellite to DEM point vector.

Sun Glint

sun_glint_lat, sun_glint_lon, sun_glint_dist

Glint location is estimated in the L1B product based on a spherical earth model. The glint location is located along the great circle arc connecting the subsatellite and subsolar points. Additionally at the glint location the satellite and solar zenith angles must be equal in order for specular reflection of sunlight to occur.

The glint calculation will be refined in a future version to use an ellipsoidal earth model.

Orbital information

asc_node_tai93, asc_node_lon, asc_node_local_solar_time, mean_anom_wrt_equat, solar_beta_angle

Spacecraft ephemeris information is used in L1B geolocation to estimate orbital parameters for use with the SGP4 simplified perturbations model. Currently a single ephemeris sample for each granule is used to perform a fixed-point iteration (see Montenbruck and Gill) to derive the model parameters. A future implementation may incorporate more ephemeris samples.

Once model parameters have been established, the SGP4 propagator is used to determine the time, longitude, and local solar time of the most recent equator crossing. Orbit phase (mean_anom_wrt_equat) is calculated based on the mean motion orbital parameter. And solar beta angle is calculated with respect to the orbital plane described via the inclination and ascending node parameters.

6.1 Coordinate Systems

No change.

6.1.1 Coordinate System Definition

No change.

6.1.2 Interferometer Optical Axis Reference (IOAR)

No change.

6.1.3 Rotating Mirror Frame (RMF)

No change.

6.1.4 Scene Selection Mirror Mounting Feet Frame (SSMF)

No change.

6.1.5 Scene Selection Module Reference (SSMR)

No change.

6.1.6 Instrument Alignment Reference (IAR)

No change.

6.1.7 Spacecraft Body Frame (SBF)

No change.

6.1.8 Orbital Coordinate System (OCS)

No change.

6.1.9 Earth Centered Inertial (ECI)

No change.

6.1.10 Earth Centered Earth Fixed (ECEF) or Earth Centered Rotating (ECR)

No change.

6.1.11 World Geodetic System 1984 (WGS84)

No change.

6.1.12 Topocentric-Horizon Coordinate System (THCS)

No change.

6.2 Coordinate System Transformations

No change.

6.3 Algorithm Partitioning

No change.

6.4 Sensor Specific Algorithm

No change.

6.4.1 CrIS FOV LOS in SSMF Coordinate System

No change.

6.4.2 SSMF to SBF Transformation Operator

No change.

6.4.3 CrIS FOV LOS in SBF Coordinate System

No change.

6.5 Spacecraft Level Algorithm

No change.

6.6 Timing Conventions

No change.

7 MODULES DEFINITION

This section summarizes the key processing steps necessary to transform L1A into L1B. The overall processing chain can be partitioned into modules listed below.

1. Initialization
   - Software initialization, the algorithm needs a one-time initialization
2. Input Data Handling
   - Low level and configuration data handling for software
   - Calibration and science data handling
3. Preprocessing
   - Interferogram to spectrum transformation
   - Moving average handling
   - Non-Linearity Correction
4. Spectral Calibration
   - Laser wavelength calibration from neon lamp data
   - Laser wavelength drift monitoring
   - Spectral axis labeling and alias unfolding
5. Radiometric Calibration
   - ICT radiance calculation
   - Complex calibration (removes instrument induced offset and phase)
   - Polarization correction (not included in v2.0, will be included in a future release)
   - Spectrum correction (correct for ILS, calibration filter, and resample to a fixed wavenumber grid)
6. Geolocation
   - FOV LOS calculation relative to spacecraft body frame
7. Quality Control
   - NEdN estimation
   - Metrology wavelength monitoring
   - Temperatures monitoring
   - Lunar intrusion detection
   - Imaginary radiance threshold tests
8. Post-processing
   - User required spectral bins selection
   - SDR data formatting
9. Output Data Handling

The conventions used in the flowcharts shown in this section are described in Figure 7.0-1.

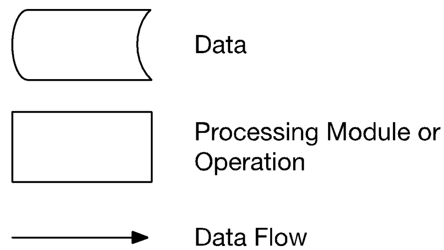

Figure 7.0-1 Conventions used in the flowcharts included in this section.

The overall processing chain required to transform raw interferograms into spectrally and radiometrically calibrated and corrected spectra is shown in Figure 7.0-2 and Figure 7.0-3. This replaces Figure 59 in the CrIS SDR ATBD.

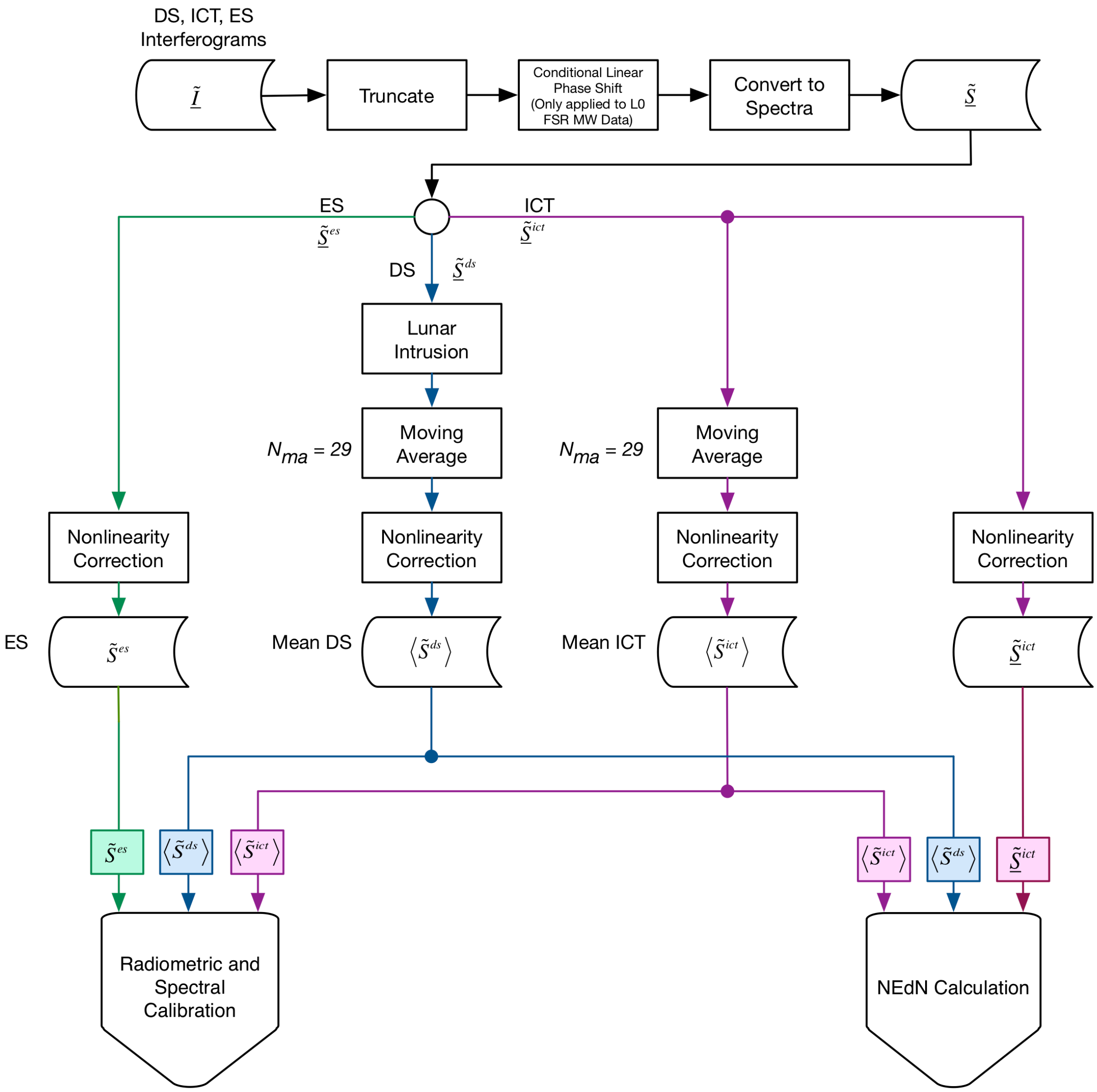

Figure 7.0-2 General flow diagram for operations performed prior to radiometric and spectral calibration.

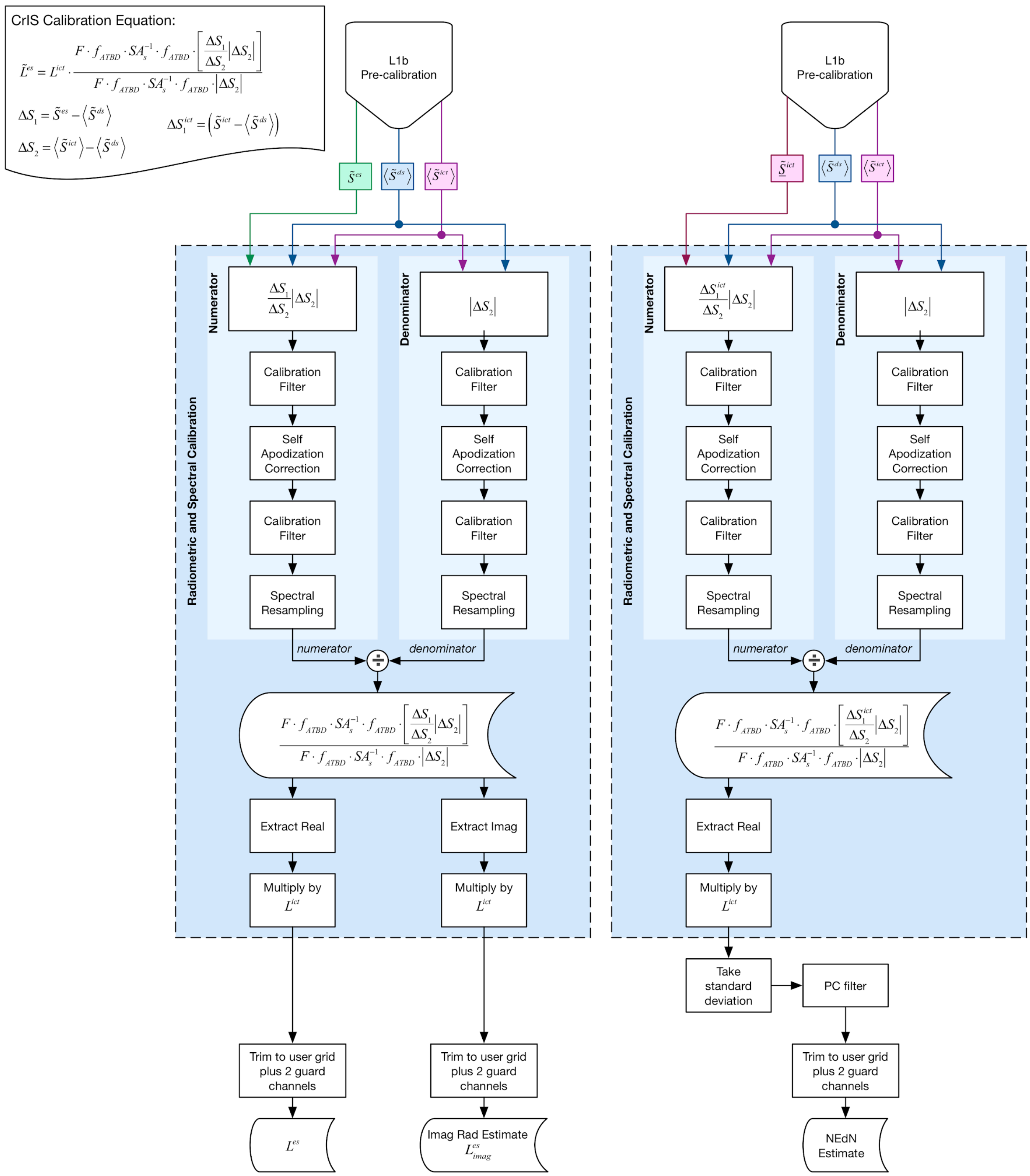

Figure 7.0-3 General flow diagram for the radiometric and spectral calibration (full calibration is used for NEdN estimates).

7.1 Initialization

The ILS curve fit parameters in the CrIS SDR ATBD (Table 17), which are intended for correction of modulation efficiency variation with OPD, are not applicable to the NASA L1B processing.

The configuration options in the CrIS SDR ATBD (Table 18: Tunable Parameters Provided via Configuration Files) that modify the processing performed by the CrIS SDR algorithm are not applicable to the NASA L1B processing. The instrument parameters that are configured within the L1B processing are listed in Table 7.1-1.

Table 7.1-1 Parameters defined in L1B processing package.

L1B mnemonic	Description
sensor.Rf	Decimation factor
sensor.An	Alias number
sensor.N	Number of points in sensor grid interferogram
sensor.iflip	spectral unfolding index
sensor.FOVangle	angle to center of FOV
sensor.FOVradius	FOV radius
sensor.startbit	FIR accumulator start bit
sensor.ModEff	
sensor.Vinst	nonlinearity correction Vinst values
sensor.a2_now	nonlinearity correction a2 coefficients
user.MOPD	Maximum Optical Path Difference (MOPD) corresponding to output resolution
user.output_range	spectral range for output data
FIRfilter.lw.h.real	LW FIR filter coefficients (real part)
FIRfilter.lw.h.imag	LW FIR filter coefficients (imag part)
FIRfilter.mw.h.real	MW FIR filter coefficients (real part)
FIRfilter.mw.h.imag	MW FIR filter coefficients (imag part)
FIRfilter.sw.h.real	SW FIR filter coefficients (real part)
FIRfilter.sw.h.imag	SW FIR filter coefficients (imag part)
invalidNeonCalibrationPercentageThreshold	neon calibration quality control parameter
computedWavelengthRejectionThreshold	neon calibration quality control parameter
c	calibration filter coefficients
fb	calibration filter frequency response
h	Planck constant used in ICT radiance calculation
k	Boltzmann constant used in ICT radiance calculation
c	speed of light constant used in ICT radiance calculation
orbit_time_vector	orbit times corresponding to SSM Baffle Offset model values in engineering packet

7.2 Input Data Handling

The implementation of data handling is consistent with the CrIS SDR ATBD. It is notable that the conversion of CCSDS packet data to "raw" interferogram observations, as well as science and engineering coefficients and measurements, is separated into a "CrIS L1A" telemetry conversion stage. That initial processing stage is not responsible for triggering science data processing activities, i.e. it is a simplified model from the "operational" implementation model described in the ATBD. L0 telemetry equivalent to RDRs is converted to L1A granules represented as files; groups of L1A granule files are then used for science SDR-equivalent L1B product generation. Granulation of CrIS data is principally done in the L1A stage of processing.

7.3 Preprocessing

The introductory section is theoretically consistent with the CrIS SDR ATBD.

7.3.1 Interferogram to Spectrum Transformation

As noted in Section 2.5.2, during the first part of the SNPP mission the effective spectral resolution of CrIS data received from the satellite was lower in the short-wave and mid-wave infrared bands than in the long-wave infrared band. Level 0 data received during this initial period is referred to as Normal Spectral Resolution (L0 NSR). On 4 December 2014 (15:06 UTC), the resolution of the short-wave and mid-wave data transmitted from the SNPP satellite was increased to match the long-wave resolution. Level 0 data received from this time through 2 November 2015 (15:48 UTC) is referred to as Full Spectral Resolution (L0 FSR). On 2 November 2015 (16:06 UTC), the satellite began transmitting long-wave and short-wave interferograms with extra points on the ends. Level 0 data received from this time forward is referred to as Extended Spectral Resolution (L0 XSR). For the NASA L1B Version 2.0 (SNPP-only) product, L1B calibrated radiance datasets are produced at two different resolutions, to meet the goals of providing a spectrally consistent product with the longest possible duration and also with the highest possible spectral resolution. These L1B datasets are referred to as NSR and FSR.

CrIS data received from the J1 satellite has been at L0 XSR for the entire mission. For the NASA L1B Version 2.11 (J1-only) product, L1B calibrated radiances are produced only at FSR.

For the L1B NSR output, the L0 FSR and L0 XSR input interferograms are truncated to L0 NSR resolution prior to transformation to spectra. Additionally, for L1B NSR output data produced from L0 Full Spectral Resolution (L0 FSR) input data, a linear phase shift is applied to the MW band complex spectra after truncation of the full resolution interferograms to low resolution interferograms. This corrects for a linear phase shift in the MW that was introduced by the onboard processing for FSR input data. This linear phase shift is not applied for NSR or XSR L0 input. For the L1B FSR dataset, no truncation or linear phase shift is applied to the XSR L0 input.

Otherwise, 7.3.1 is theoretically consistent with the CrIS SDR ATBD.

7.3.2 Moving Average Handling

This module handles the moving average of calibration target measurements (DS, ICT). Unlike the NOAA SDR algorithm, the NASA L1B algorithm uses a moving window of 29 DS and ICT measurements (14 anterior scans, the current scan, and 14 posterior scans; temperatures and spectra) are averaged per the default setting. The moving average is calculated for each scan

line, and the FIFO method described in the CrIS SDR ATBD is not used. The moving window averages for the DS and ICT are calculated using the uncalibrated spectra prior to non-linearity correction.
The NASA CrIS L1B processing does not currently support FCE detection and correction.

A general description of the moving window average process is given in Section 5.6.1.

7.3.2.1 Exception Handling

If any ICT or DS spectrum is declared invalid by CrIS sensor, lunar intrusion test or other QC measure, then the corresponding measurements are excluded from the moving window average.

If the number of valid spectra in the moving window drops below a threshold value (set such that the noise increase due to decreased average size in the reference view is less than 10%), then the “Degraded Radiometric Calibration” flag is set. If there are no valid spectra in the moving average window, then the “Invalid Radiometric Calibration” flag is set.

If a science telemetry packet is missing for a given 8-second sweep, then those telemetry values shall be excluded from the moving window average.

7.4 Spectral Calibration

No change.

7.4.1 Laser Wavelength Calibration from Neon Lamp Data

An update of metrology laser wavelength is performed for each granule based on the calibration neon count. The F-matrix resampling operator is computed separately for each granule using Neon data contained in the most coincident engineering packet. The spectral operators (calibration filter, spectral resampling, self-apodization removal) are not combined into a single CMO matrix.

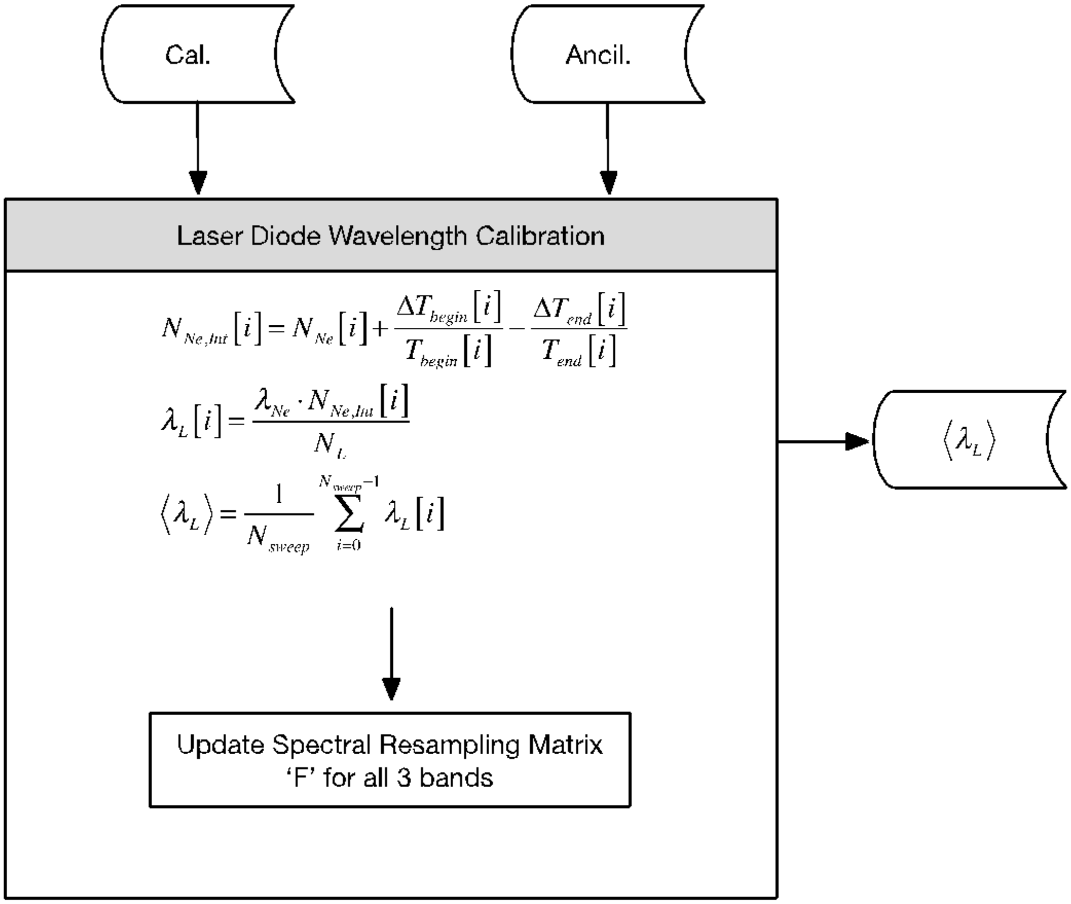

Figure 7.4.1-1 Metrology laser wavelength calibration flowchart (replaces Figure 63 in CrIS SDR ATBD).

7.4.1.1 Definition of Variables

Calibration data from engineering packet

$N_{Ne}[i]$	Integer neon fringe count from ith sweep.
$T_{begin}[i]$	Integer neon fringe count parameter from ith sweep used for interpolation.
$T_{end}[i]$	Integer neon fringe count parameter from ith sweep used for interpolation.
$\Delta T_{begin}[i]$	Integer neon fringe count parameter from ith sweep used for interpolation.
$\Delta T_{end}[i]$	Integer neon fringe count parameter from ith sweep used for interpolation.
N_{sweep}	Number of neon calibration sweeps collected & reported in engineering packet.

N_L Number of laser metrology wavelengths used to meter OPD during neon calibration sweep (N_L = 7985 always).

Ancillary data from engineering packet

λ_{Ne} Reference neon wavelength (703.44835 nm).

Local variables

$N_{Ne,Int}[i]$ Neon wavelengths counted during ith calibration sweep (non integer, interpolated).

Output variables

λ_L Average metrology laser wavelength computed from current engineering packet neon calibration data.

7.4.1.2 Exception Handling

The averaged metrology laser wavelength is computed from many neon calibration sweeps (30 is the default). Outliers are removed before the average is re-computed and reported. See section 4.1.3 of this document and the CrIS SDR ATBD, and the NASA L1B Quality Flag Description Document for more information on outlier definition and QF assertion.

7.4.2 Laser Wavelength Drift Monitoring

This section is not applicable to the NASA CrIS L1B processing software.

7.4.3 Spectral Axis Labeling and Alias Unfolding

The spectral calibration module defines the on-axis sensor spectral grid associated with each raw spectrum (band dependent), and the output spectral grid (band dependent). Based on the latest laser diode wavelength estimate, the spectral grid spacing and the minimum wavenumber of the band are computed. The raw spectrum is then rotated by the desired number of points to unfold the spectral alias that was introduced by filtering and decimation on-board the CrIS sensor. Spectral fold points have been derived for each band. The spectral unfolding yields a continuous spectrum free of alias fold points and with channel centers defined by the metrology sampling interval λ_s^b, decimation factor DF_b and the number of complex interferogram points processed N_b.

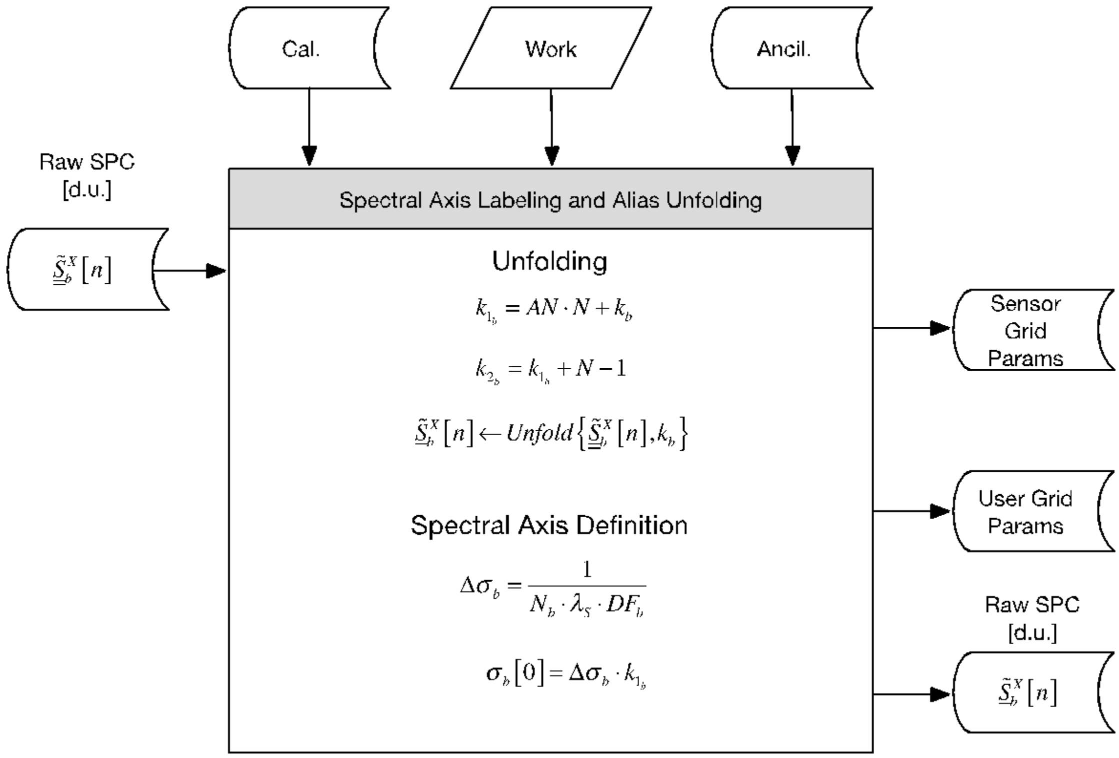

Figure 7.4.3-1 Spectral axis labeling and aliasing unfolding.

7.4.3.1 Definition of Variables

Input variables

$\tilde{\underline{\underline{S}}}_b^X[n]$ Raw complex spectrum for band ‘b’ in [d.u.] prior to spectral unfolding, corresponding to X = DS, ICT, or ES. These spectra have not yet been through non-linearity correction.

Calibration Data

λ_S Metrology sampling interval (cm) ($\lambda_s = \lambda_L/2 \approx 775x10^{-7}\,cm$). The sampling interval is half the laser metrology wavelength.

Ancillary Data

$\sigma_{0_b}^{req}$ Required minimum wavenumber channel center of first channel located in the pass band of band ‘b’ for the L1B output spectral grid (cm^{-1}).

(LW = 650.000 cm-1, MW = 1210.000 cm-1, SW = 2155.000 cm-1)

$\sigma_{1_b}^{req}$ Required maximum wavenumber channel center of last channel located in the pass band of band ‘b’ for the L1B output spectral grid (cm^{-1}).

(LW = 1095.000 cm-1, MW = 1750.000 cm-1, SW = 2550.000 cm-1)

DF_b Decimation factor for band 'b'.

AN_b Alias number for band 'b'.

k_b Index to wavenumber channel to be used for spectral unfolding.

Output variables

$\underline{\tilde{S}}_b^X[n]$ Raw complex spectrum for band 'b' in [d.u.] after spectral unfolding, corresponding to X = DS, ICT, or ES. These spectra have not yet been through non-linearity correction.

Sensor grid parameters: including interferogram sampling interval (Δx), on-axis spectral sampling interval ($\Delta\sigma$), on-axis spectral sampling grid (σ), and required minimum/maximum wavenumber channel center of first/last channel located in the pass band of band 'b' for the L1B output spectral grid ($\sigma_{0_b}^{req}, \sigma_{1_b}^{req}$)

User grid parameters: including interferogram sampling interval (Δx), on-axis spectral sampling interval ($\Delta\sigma$), on-axis spectral sampling grid (σ)

Operators

$Unfold\{V[n], k_b\}$ Shifts a complex numerical vector V according to a fold point k_b.

7.4.3.2 Exception Handling

None.

7.5 Radiometric Calibration

The CrIS specific calibration equation, as implemented by the NASA L1B CrIS processing, using notation consistent with CrIS SDR ATBD, is provided in Equation "a".

a.
$$\tilde{L}_{b,p,d}^{es}[n] = L_b^{ict}[n] \cdot \frac{F[n,n'] \cdot f_{ATBD}[n] \cdot SA_s^{-1} \cdot f_{ATBD}[n] \cdot \left[\frac{\Delta S_1}{\Delta S_2} |\Delta S_2| \right]}{F[n,n'] \cdot f_{ATBD}[n] \cdot SA_s^{-1} \cdot f_{ATBD}[n] \cdot |\Delta S_2|}$$

b.
$$\Delta S_1 = \left(\tilde{S}_{b,p,d}^{es}[n] - \left\langle \tilde{S}_{b,p,d}^{ds}[n] \right\rangle \right)$$

c.
$$\Delta S_2 = \left(\left\langle \tilde{S}_{b,p,d}^{it}[n] \right\rangle - \left\langle \tilde{S}_{b,p,d}^{ds}[n] \right\rangle \right)$$

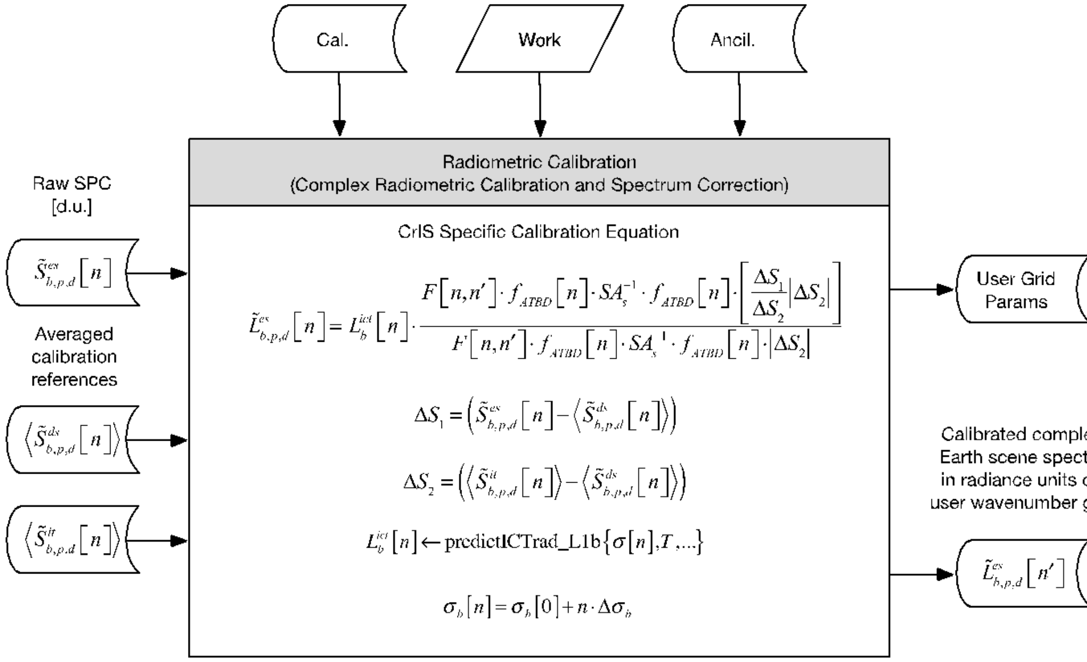

Figure 7.5-1 Radiometric calibration.

Definition of Variables
Input Variables

$\tilde{S}^{es}_{b,p,d}\left[n\right]$ Is the complex uncalibrated Earth scene spectra, expressed in [d.u.] at channel center "n", and corrected for nonlinearity.

$\left\langle \tilde{S}^{ds}_{b,p,d}\left[n\right] \right\rangle$ Is the complex uncalibrated cold reference (Deep Space) spectra averaged over N^{ma} measurements, expressed in [d.u.] at channel center "n", and corrected for nonlinearity;

$\left\langle \tilde{S}^{it}_{b,p,d}\left[n\right] \right\rangle$ Is the complex uncalibrated hot reference (ICT) spectra averaged over N^{ma} measurements, expressed in [d.u.] at channel center "n", and corrected for nonlinearity;

λ_L Average metrology laser wavelength computed from current engineering packet neon calibration data (See Section 7.4.1).

Calibration Data

See parameters in Section 7.5.2 for ICT radiance calculation.

ILS Parameters

Ancillary Data

Determined from instrument characterization. See description of ICT radiance parameters and calculation in Section 7.5.2.

N_b — Number of output spectral bins.

Work Data

See Section 7.5.2 for mean calculation of ICT telemetry components (SSM baffle temp, ICT PRT1 temp, ICT PRT2 temp, OMA1 temp, OMA temp).

Local Variables

$\sigma_b[0]$ — Wavenumber of channel having n = 0 [cm^{-1}].

$\Delta\sigma_b$ — Channel spacing [cm^{-1}].

$\sigma_b[n]$ — Wavenumber of nth channel center [cm^{-1}] (sensor wavenumber grid).

λ_S — Metrology sampling interval (cm) ($\lambda_s = \lambda_L/2 \approx 775x10^{-7}cm$). The sampling interval is half the laser metrology wavelength.

$L_b^{ict}[n]$ — Is the calculated radiance for the hot calibration reference (the ICT), calculated on the user wavenumber scale.

Operators

$F_b[n,n']$ — Is the spectral resampling matrix operator (see section 3.5);

$f_{ATBD_b}[n]$ — Is the band guard filter (see section 3.6.5);

SA_s^{-1} — Is the self-apodization removal matrix operator (see section 3.6.2);

p — Field of view (FOV);

b — Band;

d — Sweep direction;

predictICTrad_L1b{} is the function that computes the ICT predicted radiance from model inputs. (See Section 5.4 and 7.5.2 for more details).

Output Variables

$\tilde{L}_{b,p,d}^{es}[n']$ — Is the calibrated scene radiance on the user wavenumber scale;

flags — Quality flags as defined in NASA Cross Track Infrared Sounder (CrIS) Level 1B Quality Flags Description Document

7.5.1 Radiometric Complex Calibration

Radiometric calibration transforms the digital count signal into radiance units. The complex calibration method is used for the radiometric calibration process. This method also corrects for the instrument phase. Polarization correction is not included in the NASA L1B processing at this time.

Refer to Section 7.5 for the complete CrIS specific calibration equation.

7.5.1.1 Definition of Variables

Refer to Section 7.5 for the definition of variables.

7.5.1.2 Exception Handling

The sweep direction "*d*" of the ICT and DS spectra must be selected to match the sweep direction "*d*" of the Earth scene when performing radiometric complex calibration.

7.5.2 ICT Radiance Calculation

Section 7.5.2 is theoretically consistent with the CrIS SDR ATBD. However, in the NASA L1B software, the Planck radiance is computed on the on-axis sensor grid.

7.5.3 Spectrum Correction

Spectrum correction includes application of the band-guard filter, the self-apodization removal matrix operator, and the spectral resampling matrix operator. The band-guard filter is applied before and after the self-apodization removal matrix operator. All operations are applied to both the numerator and denominator of the calibration equation.

Refer to Section 7.5 for the complete CrIS specific calibration equation.

7.5.3.1 Definition of Variables

Refer to Section 7.5 for the definition of variables.

7.5.3.2 CMO Computation

The spectral operators (bandguard filter, spectral resampling, self-apodization removal, and Hamming apodization) are not combined into a single CMO matrix. Hamming apodization is not applied.

7.5.3.3 Exception Handling

N/A.

7.5.4 Non-linearity Correction

Section 7.5.4 is theoretically consistent with the CrIS SDR ATBD.

7.6 Quality Control

No change.

7.6.1 NEdN Estimation

The NEdN estimate is based on ICT measurements that have been collected within the moving window averaging interval. The default width of the averaging window is 29 scans ($N^{ma} = 29$) which corresponds to 14 anterior scans, the current scan, and 14 posterior scans.

The calibrated ICT measurements provide ability to calculate an NEdN estimate based on the stable ICT target temperature. Principal component filtering is employed to spectrally smooth the NEdN estimate. The NEdN estimate is calculated on the sensor wavenumber grid, using the full radiometric and spectral complex calibration and then interpolated to the output SDR wavenumber grid.

The NEdN calculation uses ICT spectra in place of Earth scene spectra in the radiometric complex calibration and the spectra are not corrected for nonlinearity.

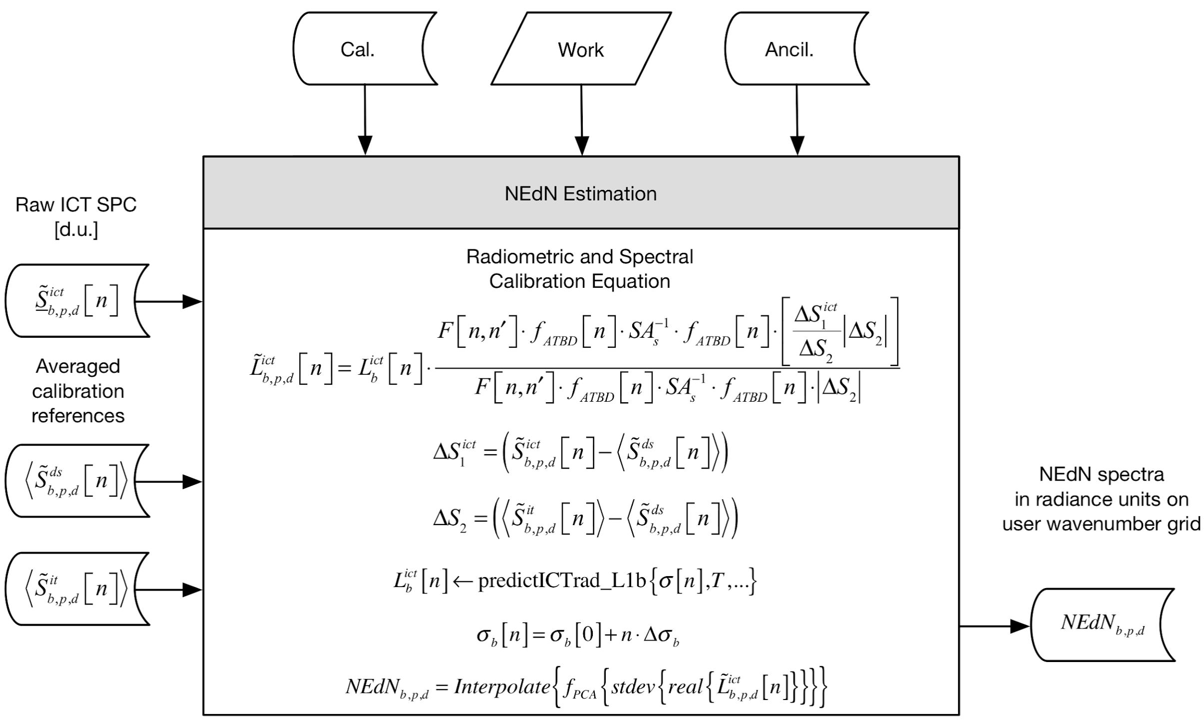

Figure 7.6.1-1 NEdN estimation flowchart.

7.6.1.1 Definition of Variables

Input Variables

$\underline{\tilde{S}}^{ict}_{b,p,d}\left[n\right]$ Complex uncalibrated ICT spectra, expressed in [d.u.] at channel center "n", and uncorrected for nonlinearity.

$\left\langle \tilde{S}^{ds}_{b,p,d}\left[n\right]\right\rangle$ Is the complex uncalibrated cold reference (Deep Space) spectra averaged over N^{ma} measurements, expressed in [d.u.] at channel center "n", and corrected for nonlinearity.

$\left\langle \tilde{S}^{it}_{b,p,d}\left[n\right]\right\rangle$ Is the complex uncalibrated hot reference (ICT) spectra averaged over N^{ma} measurements, expressed in [d.u.] at channel center "n", and corrected for nonlinearity.

Calibration data from engineering packet

See parameters in Section 7.5.2 for ICT radiance calculation.

Work variables

See Section 7.5.2 for mean calculation of ICT telemetry components (SSM baffle temp, ICT PRT1 temp, ICT PRT2 temp, OMA1 temp, OMA temp).

Local variables

$\sigma_b\left[0\right]$ Wavenumber of channel having n = 0 [cm^{-1}]';

$\Delta\sigma_b$ Channel spacing [cm^{-1}];

$\sigma_b\left[n\right]$ Wavenumber of nth channel center [cm^{-1}] (sensor wavenumber grid);

λ_S Metrology sampling interval (cm) ($\lambda_s = \lambda_L/2 \approx 775x10^{-7}\,cm$). The sampling interval is half the laser metrology wavelength;

$L^{ict}_b\left[n\right]$ Is the calculated radiance for the hot calibration reference (the ICT), calculated on the user wavenumber scale;

$\tilde{L}^{ict}_{b,p,d}\left[n\right]$ Complex calibrated ICT radiance;

p Field of view (FOV);

b Band;

d Sweep direction.

Output variables

$NEdN_{b,p,d}$ NEdN estimate for nth channel on SDR wavenumber output grid.

7.6.2 Fringe Count Error Handling

Not implemented in this version.

7.6.3 Fringe Count Error Detection

Not implemented in this version.

7.6.4 Fringe Count Error Correction

Not implemented in this version.

7.6.5 Data Quality Indicators

The NASA L1B software produces Quality Flag (QF) variables describing the quality of the primary data products. The individual flags in the QF variables are specific to the CrIS L1B algorithm and therefore are different from the flags in the SDR product.

For guidance on using QFs, refer to the "NASA Cross Track Infrared Sounder (CrIS) Level 1B Product Users' Guide, Version 2.11".

For detailed information regarding the derivation and meaning of the individual flags that make up the CrIS L1B QF variable, refer to the "NASA Cross-track Infrared Sounder (CrIS) Level 1B Quality Flags Description Document, Version 2.11". This document includes a mapping of the individual CrIS SDR quality flags to CrIS L1B quality flags where applicable.

7.7 Post-Processing

N/A.

7.7.1 User Required Spectral Bins Selection

N/A.

7.7.2 SDR Data Formatting

N/A.

7.8 Output Data Handling

The format of the CrIS L1B product is described in the NASA Cross Track Infrared Sounder (CrIS) Level 1B Product Users' Guide, Version 2.11.

8 CONCLUSION

The CrIS SDR ATBD defines the Level 1B algorithms needed on the ground in order to produce meaningful data meeting all the requirements of the CrIS instrument. This document identifies only the changes to the CrIS SDR ATBD document necessary to describe the algorithm used to produce the Version 2.11 NASA CrIS L1B radiance data product.

9 APPENDICES

9.1 Fast Fourier Transforms

No change.

9.1.1 Comments on Various Algorithms

No change.

9.1.2 Data Translation and Centering

No change.

9.1.3 Prime Factor Algorithm Fast Fourier Transform

No change.

9.2 Alias Unfolding

No change.

9.3 Linear Fitting

No change.

9.3.1 Implementation of the Linear Interpolation

No change.

9.4 Numerical Integration

No change.

9.5 Determination of the Goodness of Fit

No change.

9.6 Definitions

No change.

9.6.1 Sensor Calibration

No change.

9.6.2 Raw Data Record (RDR)

No change.

9.6.3 Sensor Data Record (SDR)

No change.

9.6.4 Environmental Data Record (EDR)

No change.

9.6.5 Data Product Levels

No change.

9.6.6 Measured Data

No change.

9.6.7 Auxiliary Data

No change.

9.6.8 Ancillary Data

The CrIS L1B algorithm requires Leap Seconds and UTC Polar Wander files. These requirements are described in the "CrIS L1B Software User's Guide, Version 2.1".

9.6.9 Other Instrument Specific Terms and Definitions

No change.

— End of document —